Frequency-stabilized cavity ring-down spectroscopy measurements of carbon dioxide isotopic ratios

D. A. Long[1], M. Okumura[1], C. E. Miller[2] and J. T. Hodges[3,*]
[1]*Division of Chemistry and Chemical Engineering, California Institute of Technology, Pasadena, CA 91125, USA*
[2]*Jet Propulsion Laboratory, California Institute of Technology, 4800 Oak Grove Drive, Pasadena, CA 91109, USA and*
[3]*Chemical and Biochemical Reference Data Division, National Institute of Standards and Technology, 100 Bureau Drive, Gaithersburg, Maryland 20899, USA*
(Dated: August 27, 2010)

*Corresponding author:
Email address: joseph.hodges@nist.gov (J. T. Hodges) Tel.: +1(301)975-2605; fax: +1(301)869-5924.

Abstract
Carbon dioxide (CO_2) isotopic ratios were measured at 1.6 μm through the use of frequency-stabilized cavity ring-down spectroscopy (FS-CRDS). We report the highest spectrum signal-to-noise ratios to date for CO_2 transitions, with values as high as 28,000:1 achieved. Measured single-spectrum precisions were 0.11‰, 0.09‰, and 0.59‰ for the $^{13}C/^{12}C$, $^{18}O/^{16}O$, and $^{17}O/^{16}O$ ratios, respectively. In addition, the importance of utilizing the Galatry line profile is demonstrated. The use of the Voigt line profile, which neglects the observed collisional narrowing, leads to large systematic errors which are transition-dependent and vary with temperature and pressure. While the low intensities of CO_2 transitions at 1.6 μm make this spectral region non-optimal, the sensitivity and stability of FS-CRDS have enabled isotope ratio measurement precisions comparable with other optical techniques which operate at far more propitious wavelengths. These results indicate that a FS-CRDS spectrometer constructed at 2.0 or 4.3 μm could achieve significantly improved precision over the present instrument and likely be competitive with mass spectrometric methods.

1. Introduction
For over half of a century, stable isotope measurements have been utilized to quantify sources and sinks of CO_2 [1]. Recent simultaneous measurements of $^{18}O/^{16}O$ and $^{17}O/^{16}O$ isotopic ratios have elicited considerable interest due to their use as a tracer of stratospheric dynamics through the observed mass-independent isotope effect [2]. In addition, isotopic fractionation measurements are important in partitioning CO_2 emissions between natural and anthropogenic sources and deducing exchange between the biosphere, ocean, and atmosphere [3].

Isotope-ratio mass spectrometry (IR-MS) is the standard for isotope fractionation measurements. Commercial, dual-beam IR-MS instruments routinely achieve measurement precisions better than 0.1‰ for measurements of $^{13}C/^{12}C$ and $^{18}O/^{16}O$ isotopic ratios (e.g. [4]). Unfortunately, IR-MS has its share of technical limitations: it is expensive, bulky, time-intensive, sample destructive, and requires careful sample preconcentration to remove isobaric interferences. In addition, IR-MS analysis is not compatible with sticky molecules such as H_2O and SO_2; thus, isotopic analysis of these species requires an initial chemical conversion which greatly increases the complexity and overall uncertainty of the measurement. Finally, measurements of $^{17}O/^{16}O$ ratios in

CO_2 by IR-MS are greatly complicated by the presence of the $^{16}O^{13}C^{16}O$ isobar. This necessitates an initial conversion of CO_2 to O_2 which introduces an uncertainty of ~±0.1‰ and precludes a simultaneous measurement of the $^{13}C/^{12}C$ ratio [5].

These IR-MS difficulties have led to the development of laser-based isotope ratios measurements [6]. Laser-based absorption techniques have significant potential for inexpensive, *in situ* measurements. In addition, since individual isotopologues exhibit distinct spectra, laser-based isotope measurements are not susceptible to isobaric interference. As these techniques have recently been reviewed [6-7], we will only discuss a few recent developments in laser-based isotope ratio measurements. For measurements of $^{13}C/^{12}C$ ratios, laser-based techniques have begun to rival IR-MS, with commercially-available instruments offering precisions better than 0.3‰. For $^{18}O/^{16}O$ precisions as high as 0.05‰ have been achieved through the use of quantum cascade lasers which can access the CO_2 fundamental band at 4.3 μm [8]. The low isotopic abundance of $^{16}O^{12}C^{17}O$ presents a significant challenge to spectroscopic measurements (see Table 1 for natural isotopic abundances). As a result, only three previous studies have measured the $^{17}O/^{16}O$ isotopic ratio of CO_2 [9-11] . The highest precision was achieved by Castrillo et al. [11] utilizing wavelength-modulation spectroscopy with a liquid-nitrogen-cooled quantum cascade laser emitting at 4.3 μm. Short term precisions of 0.5‰ and 0.6‰ were achieved for the $^{18}O/^{16}O$ and $^{17}O/^{16}O$ isotopic ratios, respectively. Unfortunately, the measurements exhibited large, systematic deviations of 11.5‰ and -13.0‰ for the two isotopic ratio measurements, respectively. These were attributed to either non-linearity in the second-harmonic detection (as they were operating outside of the linear Beer's law regime) or non-linearity in their HgCdTe detector.

We have recently constructed a frequency-stabilized cavity ring-down spectrometer in order to perform ultrasensitive, high-resolution lineshape studies of CO_2 in the near-infrared at 1.6 μm [12]. These laboratory measurements will assist remote sensing measurements of atmospheric CO_2 concentrations [13-14]. We have taken this opportunity to evaluate the potential of frequency-stabilized cavity ring-down spectroscopy (FS-CRDS) for measurements of CO_2 isotopic ratios. While this wavelength range is non-optimal due to the relative weakness of these transitions (two orders of magnitude weaker than the transitions at 2.0 μm and five orders of magnitude weaker than the fundamental at 4.3 μm), this study will allow us to compare FS-CRDS to other optical methods in the determination of isotopic ratios. In addition, the results of this study will allow us to estimate the precision and accuracy of a FS-CRDS measurements made at a more advantageous wavelength.

2. Experimental Apparatus

Measurements were made using the frequency-stabilized cavity ring-down spectrometer located at the National Institute of Standards and Technology (NIST) in Gaithersburg, MD. The FS-CRDS spectrometer utilized herein is similar to the FS-CRDS instrument which has previously been employed to measure the O_2 *A*-band at 0.762 μm [15-22]. The significant change has been the use of an external-cavity diode laser whose output is centered at 1.6 μm, thus, allowing us to access CO_2 transitions in near-infrared wavelengths. This change in spectral region required the use of a different pair of highly-reflective mirrors and an InGaAs detector. All aspects of the locking and data collection

methods were identical for the two instruments. Due to the similarities of the two instruments; we will only present the most pertinent details in this publication.

FS-CRDS differs from traditional cw-cavity ring-down spectroscopy in two fundamental ways [23-24]. Firstly, the optical cavity length is actively stabilized to an external frequency reference, in our case a frequency-stabilized HeNe with a long-term stability of 1 MHz (3×10^{-5} cm^{-1}) over 8 h. Secondly, FS-CRDS is a single-mode cavity ring-down technique. Individual cavity resonances are selectively excited, allowing for accurate, quantitative measurements. During a spectral scan, the probe laser frequency is locked to successive TEM_{00} cavity modes with ring-down time constants collected at each frequency step. This leads to an extremely stable, accurate, and linear frequency axis. We have recently demonstrated the capability to measure line positions with uncertainties less than 0.5 MHz (1.5×10^{-5} cm^{-1}) [15], Doppler (Gaussian) widths to better than 1 part in 6,000 [20], and line intensities with uncertainties less than 0.3% [17,22]. Importantly, the FS-CRDS spectrometer is completely automated such that spectra can be taken over a broad spectral region without operator intervention [24].

The probe source was an external-cavity diode laser with a tuning range of 1.57-1.63 μm and an output power of 15-18 mW. The ring-down cavity mirrors had nominal reflectivities of 99.997%, corresponding to a finesse of ~105,000 and an effective pathlength of ~25 km. The relative standard deviation of the measured ring-down time constant was ~0.05%, which for these mirrors and cavity length leads to a minimum detectable absorption coefficient of 2.1×10^{-10} cm^{-1}. Given an acquisition rate of 30 Hz, the noise-equivalent absorption coefficient was 3.8×10^{-11} cm^{-1} $Hz^{-1/2}$. The cavity's free spectral range was determined to be 203.097(22) MHz via the procedure of Lisak et al. [25].

The FS-CRDS system stability was assessed through a measurement of the Allan variance [26], a measure which was originally derived as a performance metric for atomic clock standards. Figure 1 shows that as successive ring-down time constants are averaged the Allan deviation (square-root of the Allan variance) decreases in a roughly ergodic manner. After averaging ~3,000 ring-down time constants the Allan variance reaches a minimum, indicating the presence of system drifts on the ~100 s time-scale. The use of 3,000 averages leads to an uncertainty in the absorption coefficient of 1.5×10^{-11} cm^{-1}, a fifteen-fold decrease relative to the single-shot case. For the measurements discussed herein 300 averages were employed.

Measurements were made on a sample of pure CO_2 at natural isotopic abundance and a nominal pressure of 6.67 kPa (50 Torr). Pressure measurements were made with a NIST-calibrated capacitance diaphragm gauge with a relative standard uncertainty of less than 0.1% and a full-scale response of 133 kPa (1,000 Torr). Temperature was measured through the use of a NIST-calibrated 2.4 kΩ thermistor. Spectra were collected at room temperature (298.60-299.22 K) with no attempt made to actively control the cell temperature.

3. Results and Discussion

Measurements were made in the 6263-6271 cm^{-1} wave number region (see Fig. 2). This spectral region was selected since it provides transitions from multiple isotopologues with comparable absorption. This allows us to make the most precise measurements of the isotopic ratios [27-29]. One disadvantage of this approach is that isotopologue

transitions of comparable absorption typically have very different lower state energies and, therefore, different temperature dependencies. The uncertainty in the measured isotopic ratio, u_δ, due to the temperature uncertainty, u_T, can be calculated as [28]:

$$u_\delta \approx \frac{\Delta E''}{kT}\frac{u_T}{T} \quad (1)$$

where $\Delta E''$ is the difference in lower state energies of the pair of transitions probed, T is the temperature, and k is the Boltzmann constant. It has been shown that the temperature uncertainty in these FS-CRDS measurements is ~28 mK [19]. For the $^{16}O^{13}C^{16}O$, $^{16}O^{12}C^{18}O$, and $^{16}O^{12}C^{17}O$ isotopologue transitions utilized in the present study (see Table 1), this temperature uncertainty leads to Type *B* (systematic) uncertainties in the isotopic ratio measurements of ~0.47‰, ~0.83‰ and ~0.70‰, respectively.

Figure 2 shows a spectral survey of the 6263-6271 cm^{-1} region and a spectrum which was calculated using the Voigt line profile parameters found in the HITRAN 2008 database [30]. Approximately 170 transitions were observed in this survey representing the $^{16}O^{12}C^{16}O$, $^{16}O^{13}C^{16}O$, $^{16}O^{12}C^{18}O$, $^{16}O^{12}C^{17}O$, $^{16}O^{13}C^{18}O$ isotopologues with intensities ranging from 7.8×10^{-26} to 3.6×10^{-29} cm molec.$^{-1}$. All detected transitions were found in the HITRAN 2008 database with the exception of the $^{16}O^{13}C^{16}O$ (14411)←(00001) *R*38 transition. This transition is listed in the database of Perevalov et al. [31] with an intensity of $S\sim3.04\times10^{-28}$ cm molec.$^{-1}$.

All spectral transitions were fit with a Galatry lineshape [32] which accounts for Dicke (collisional) narrowing [33]. The Doppler width was constrained to the theoretical value based upon the measured temperature, while the other parameters were floated during the resulting fit. It should be noted that the use of the Galatry profile (as opposed to the commonly used Voigt profile) is critical for this application. The use of the Voigt profile incurs large, systematic residuals due to a failure to account for collisional narrowing (see Fig. 3).

Moreover, the use of the Voigt profile also results in a measured area (and therefore concentration) which is on average ~20‰ lower than with the Galatry profile, an error which is far greater than our experimental uncertainty. The difference in areas measured using the two line profiles is not identical for the considered isotopologue transitions but rather varies between 10‰ and 40‰, thus, removing the possibility of a constant correction factor. This is not surprising as collisional narrowing parameters are known to exhibit *J*-dependence (e.g. [22,34-35]). In addition, this deviation is expected to be both pressure and temperature dependent.

Importantly, the diffusion coefficient, and therefore, (roughly) the collisional narrowing parameter, for pure CO_2 is considerably lower than for CO_2 in air (0.09 vs. 0.14 cm^2 s^{-1} at 273 K and 101.3 kPa [36]). As a result, the observed deviation between the Voigt and Galatry profiles would be expected to be even larger in a natural abundance CO_2 sample. We have experimentally verified this prediction for the air-broadened $^{16}O^{12}C^{16}O$ *R*16 (30012)←(00001) transition where the difference in fitted areas derived using the Voigt and Galatry line profiles is as much as 75‰ at 6.67 kPa [12].

An example spectrum of the $^{16}O^{12}C^{16}O$ *R*66 (30013)←(00001) transition (at natural isotopic abundance in a pure CO_2 sample at 6.67 kPa and 298.929 K) and the corresponding Galatry fit can be found in Fig. 3. This transition is located at 6263.369778

cm^{-1} with an intensity of 3.156×10^{-26} cm molec.$^{-1}$ [30]. The signal-to-noise ratio (SNR, defined as the ratio of peak absorption to root-mean-square fit residuals) is 28,000:1, leading to a precision in the area measurement of 0.03‰. This is the highest SNR ever reported for a CO_2 transition. The highest SNR previously reported was ~10,000:1 by Casa et al. [34] who utilized an intensity-stabilized diode laser absorption spectrometer to probe transitions at 2.0 μm. Note that the transition shown in Fig. 3 is ~40,000 times weaker than the transitions probed in the Casa et al. study.

Figure 4 shows an example spectrum of one of the doubly-substituted CO_2 isotopologues, $^{16}O^{13}C^{18}O$, with a SNR of 20:1. Note that interfering transitions have been fitted and subtracted from the shown spectrum. This transition is located at 6270.3543 cm^{-1} with an intensity of only 3.588×10^{-29} cm molec.$^{-1}$ at natural isotopic abundance [30]. The Type *A* (random) uncertainty of the measured area resulting from the Galatry fit is ~50‰, demonstrating the capability of FS-CRDS to make quantitative measurements of ultra-weak absorption features. This transition is eleven orders of magnitude weaker than $^{16}O^{12}C^{16}O$ fundamental transitions in the mid-infrared and is one of the weakest transitions to be quantitatively measured in the laboratory. Unfortunately, this precision pales in comparison to modern IR-MS measurements, which can achieve external precisions as high as 0.01‰ for this isotopologue through the use of large, preconcentrated samples and long averaging times (~24 h) [37].

We found single-spectrum fit precisions of 0.11‰, 0.09‰ and 0.59‰ for the $^{13}C/^{12}C$, $^{18}O/^{16}O$ and $^{17}O/^{16}O$ ratios, respectively. These single-spectrum precisions were calculated based upon the spectral SNR of the fitted spectra and therefore do not include systematic uncertainties. They represent the highest precision which could be achieved with the present instrument, for transitions of the given line intensities, in the absence of confounding effects such as temperature uncertainties and interfering transitions. The corresponding uncertainties due to temperature can be calculated, as shown in (1). Once added in quadrature with the shown single-spectrum fit precisions, the corresponding uncertainties are 0.35‰, 0.70‰ and 0.80‰ for the $^{13}C/^{12}C$, $^{18}O/^{16}O$ and $^{17}O/^{16}O$ ratios, respectively.

The presence of interfering transitions, which leads to additional unconstrained fit parameters and a more weakly constrained area determination, can degrade the reproducibility of the isotope ratio measurement. In order to quantify the magnitude of this effect, several repeated measurements of the chosen isotopologue transitions were performed to measure the distribution of fitted areas. During these fits, the pressure broadening and collisional narrowing parameters were held fixed to our previously measured values. For the $^{16}O^{13}C^{16}O$, $^{16}O^{12}C^{18}O$ and $^{16}O^{12}C^{17}O$ transitions the relative standard deviations of the ensemble of measured areas were 4‰, 0.5‰, and 10‰, respectively. For the $^{16}O^{12}C^{18}O$ transition this uncertainty is lower than the previously estimated precision, indicating that neighboring transitions play a negligible role in this measurement. This was to be expected as all neighboring transitions are orders of magnitude weaker than the $^{16}O^{12}C^{18}O$ transition in this spectral region. However, for the $^{16}O^{13}C^{16}O$ and $^{16}O^{12}C^{17}O$ transitions, it is clear that neighboring transitions significantly impact the reproducibility of the isotopic ratio. Thus, the dominant uncertainty in the $^{18}O/^{16}O$ measurement is due to temperature while for the $^{13}C/^{12}C$ and $^{17}O/^{16}O$ measurements it is due to the presence of interfering transitions.

This suggests two areas in which the precision of a future FS-CRDS based isotope ratio measurement could be improved. Firstly, the introduction of active temperature control to minimize the temperature gradient is needed if the $^{18}O/^{16}O$ measurement is to be improved. For example, by reducing the temperature uncertainty to the few mK-level, the uncertainty in the isotopic ratio measurement due to temperature, u_δ, could be reduced below the single-spectrum fit precision. Secondly, by moving to a more optimal wavelength range we could access transitions which are orders of magnitude stronger (two orders of magnitude for 2.0 μm or five orders of magnitude for 4.3 μm). Distributed-feedback diode lasers are readily available at 2.0 μm and external-cavity quantum-cascade lasers (which operate without cryogenic cooling) are now available at 4.3 μm. By moving to 2.0 μm, the stronger transitions would allow us to utilize a lower pressure in our measurements, where the relevant isotopologue transitions would be significantly more isolated. This would eliminate the dominant uncertainty in the $^{13}C/^{12}C$ and $^{17}O/^{16}O$ measurements. In addition, the spectral SNRs for the $^{16}O^{12}C^{17}O$ and $^{16}O^{13}C^{18}O$ transitions would be significantly higher due to the increased intensities in this range. It is worth noting that this would not be the case for the $^{16}O^{12}C^{16}O$ and $^{16}O^{12}C^{18}O$ transitions where we are already utilizing nearly the complete dynamic range of the instrument. The use of the fundamental band at 4.3 μm would lead to an additional three orders of magnitude increase in spectral intensity and allow for CO_2 isotope ratios to be measured at natural abundance (i.e. ~385 ppm) with precisions similar to those discussed for pure CO_2 at 2.0 μm.

4. Conclusions

Frequency-stabilized cavity ring-down spectroscopy (FS-CRDS) was employed to optically measure CO_2 isotopic ratios at 1.6 μm. Although this spectral region is non-optimal, the sensitivity and stability of FS-CRDS led to single-spectrum fit precisions of 0.20‰, 0.09‰ and 0.59‰ for the $^{13}C/^{12}C$, $^{18}O/^{16}O$ and $^{17}O/^{16}O$ ratios, respectively. $^{16}O^{12}C^{16}O$ transitions were measured with signal-to-noise ratios (SNRs) as high as 28,000:1, corresponding to the highest SNR ever reported for CO_2. Due to the presence of collisional narrowing, the use of Voigt line profiles significantly compromises the accuracy of the measured isotopic ratios. The fitted areas derived using the two line profiles differ by 10-40‰ for the measured transitions, which is far greater than the experimental precision. Future developments will focus upon the 2.0 μm band where transitions are several orders of magnitude stronger than those discussed herein and are readily accessible through the use of distributed feedback diode lasers. This should enable simultaneous measurements of $^{13}C/^{12}C$, $^{18}O/^{16}O$, and $^{17}O/^{16}O$ with sub-0.5‰ total uncertainties.

Acknowledgements

David A. Long was supported by the National Science Foundation and National Defense Science and Engineering Graduate Fellowships. Part of the research described in this paper was performed at the Jet Propulsion Laboratory, California Institute of Technology, under contract with the National Aeronautics and Space Administration (NASA). Additional support was provided by the Orbiting Carbon Observatory (OCO) project, a NASA Earth System Science Pathfinder (ESSP) mission; the NASA Upper Atmospheric

Research Program grant NNG06GD88G and NNX09AE21G; and the NIST Greenhouse Gas Measurements and Climate Research Program.

References

[1] M. H. Thiemens, Science **283,** 341-345 (1999).
[2] D. Krankowsky, F. Bartecki, G. G. Klees, K. Mauersberger, K. Schellenbach, J. Stehr, Geophys. Res. Lett. **22,** 1713-1716 (1995).
[3] P. Ghosh, W. A. Brand, Int. J. Mass Spectrom. **228,** 1-33 (2003).
[4] W. Brand, In: *Handbook of Stable Isotope Analytical Techniques*, Ed. by P.A. de Groot (Elsevier, Amsterdam, 2004), Chapt. 38.
[5] S. K. Bhattacharya, M. H. Thiemens, Z. Naturfors. **44,** 435-444 (1989).
[6] E. Kerstel, L. Gianfrani, Appl. Phys. B **92,** 439-449 (2008).
[7] E. R. T. Kerstel, In: *Handbook of Stable Isotope Analytical Techniques*, Ed. by P.A. de Groot (Elsevier, Amsterdam, 2004), Chapt. 34.
[8] B. Tuzson, J. Mohn, M. J. Zeeman, R. A. Werner, W. Eugster, M. S. Zahniser, D. D. Nelson, J. B. McManus, L. Emmenegger, Appl. Phys. B-Lasers Opt. **92,** 451-458 (2008).
[9] B. Lehmann, M. Wahlen, R. Zumbrunn, H. Oeschger, Appl. Phys. **13,** 153-158 (1977).
[10] K. P. Petrov, R. F. Curl, F. K. Tittel, Appl. Phys. B **66,** 531-538 (1998).
[11] A. Castrillo, G. Casa, L. Gianfrani, Opt. Lett. **32,** 3047-3049 (2007).
[12] D. A. Long, D. K. Havey, K. Bielska, M. Okumura, C. E. Miller, J. T. Hodges**,** In preparation (2010).
[13] D. Crisp, R. M. Atlas, F. M. Breon, L. R. Brown, J. P. Burrows, P. Ciais, B. J. Connor, S. C. Doney, I. Y. Fung, D. J. Jacob, C. E. Miller, D. O'Brien, S. Pawson, J. T. Randerson, P. Rayner, R. J. Salawitch, S. P. Sander, B. Sen, G. L. Stephens, P. P. Tans, G. C. Toon, P. O. Wennberg, S. C. Wofsy, Y. L. Yung, Z. Kuang, B. Chudasama, G. Sprague, B. Weiss, R. Pollock, D. Kenyon, S. Schroll, *Trace Constituents in the Troposphere and Lower Stratosphere* (Pergamon-Elsevier Science Ltd, Kidlington, 2004, 700-709).
[14] M. Yokomizo, Fujitsu Sci. Tech. J. **44,** 410-417 (2008).
[15] D. J. Robichaud, J. T. Hodges, P. Maslowski, L. Y. Yeung, M. Okumura, C. E. Miller, L. R. Brown, J. Mol. Spectrosc. **251,** 27-37 (2008).
[16] D. J. Robichaud, J. T. Hodges, D. Lisak, C. E. Miller, M. Okumura, J. Quant. Spectrosc. Radiat. Transf. **109,** 435-444 (2008).
[17] D. J. Robichaud, J. T. Hodges, L. R. Brown, D. Lisak, P. Maslowski, L. Y. Yeung, M. Okumura, C. E. Miller, J. Mol. Spectrosc. **248,** 1-13 (2008).
[18] D. J. Robichaud, L. Y. Yeung, D. A. Long, M. Okumura, D. K. Havey, J. T. Hodges, C. E. Miller, L. R. Brown, J. Phys. Chem. A **113,** 13089 (2009).
[19] D. K. Havey, D. A. Long, M. Okumura, C. E. Miller, J. T. Hodges, Chem. Phys. Lett. **483,** 49-54 (2009).
[20] D. A. Long, D. K. Havey, M. Okumura, H. M. Pickett, C. E. Miller, J. T. Hodges, Phys. Rev. A **80,** 042513 (2009).
[21] D. A. Long, D. K. Havey, M. Okumura, C. E. Miller, J. T. Hodges, Phys. Rev. A **81,** 064502 (2010).

[22] D. A. Long, D. K. Havey, M. Okumura, C. E. Miller, J. T. Hodges, J. Quant. Spectrosc. Radiat. Transfer **111,** 2021-2036 (2010).
[23] J. T. Hodges, H. P. Layer, W. W. Miller, G. E. Scace, Rev. Sci. Instrum. **75,** 849-863 (2004).
[24] J. T. Hodges, R. Ciurylo, Rev. Sci. Instrum. **76** (2005).
[25] D. Lisak, J. T. Hodges, Appl. Phys. B **88,** 317-325 (2007).
[26] D. W. Allan, Proc. IEEE **54,** 221-231 (1966).
[27] J. F. Becker, T. B. Sauke, M. Loewenstein, Appl. Opt. **31,** 1921-1927 (1992).
[28] P. Bergamaschi, M. Schupp, G. W. Harris, Appl. Opt. **33,** 7704-7716 (1994).
[29] G. Gagliardi, A. Castrillo, R. Q. Iannone, E. R. T. Kerstel, L. Gianfrani, Appl. Phys. B **77,** 119-124 (2003).
[30] L. S. Rothman, I. E. Gordon, A. Barbe, D. C. Benner, P. F. Bernath, M. Birk, V. Boudon, L. R. Brown, A. Campargue, J. P. Champion, K. Chance, L. H. Coudert, V. Dana, V. M. Devi, S. Fally, J. M. Flaud, R. R. Gamache, A. Goldman, D. Jacquemart, I. Kleiner, N. Lacome, W. J. Lafferty, J. Y. Mandin, S. T. Massie, S. N. Mikhailenko, C. E. Miller, N. Moazzen-Ahmadi, O. V. Naumenko, A. V. Nikitin, J. Orphal, V. I. Perevalov, A. Perrin, A. Predoi-Cross, C. P. Rinsland, M. Rotger, M. Simecková, M. A. H. Smith, K. Sung, S. A. Tashkun, J. Tennyson, R. A. Toth, A. C. Vandaele, J. Vander Auwera, J. Quant. Spectrosc. Radiat. Transfer **110,** 533-572 (2009).
[31] B. V. Perevalov, V. I. Perevalov, A. Campargue, J. Quant. Spectrosc. Radiat. Transf. **109,** 2437-2462 (2008).
[32] L. Galatry, Phys. Rev. **122,** 1218-1223 (1961).
[33] R. H. Dicke, Phys. Rev. **89,** 472-473 (1953).
[34] G. Casa, R. Wehr, A. Castrillo, E. Fasci, L. Gianfrani, J. Chem. Phys. **130,** 184306 (2009).
[35] R. Wehr, R. Ciurylo, A. Vitcu, F. Thibault, J. R. Drummond, A. D. May, **235,** 54-68 (2006).
[36] J. O. Hirschfelder, C. F. Curtiss, R. B. Bird, *Molecular Theory of Gases and Liquids* (Wiley, New York, 1954, 579-581).
[37] K. W. Huntington, J. M. Eiler, H. P. Affek, W. Guo, M. Bonifacie, L. Y. Yeung, N. Thiagarajan, B. Passey, A. Tripati, M. Daeron, R. Came, J. Mass Spectrom. **44,** 1318-1329 (2009).

TABLE 1 CO_2 isotopologue transitions utilized in this study. Positions, intensities (at natural isotopic abundance [30], n_a, and T=296 K), and lower state energies (E'') are from the HITRAN 2008 database [30]. The shown Type *A* (random) uncertainties capture the Galatry fit uncertainty as calculated based upon the spectral signal-to-noise ratio (SNR). The uncertainty in the corresponding ratio measurement due to temperature, u_δ, is a Type *B* (systematic) uncertainty which was calculated as shown in (1). Note that the uncertainties in p and the free spectral range are not present as these will cancel in the isotopic ratio measurements. The quantity $A_{Diff} = 1000(A_{GP}/A_{VP}-1)$, where A_{GP} and A_{VP} are the spectral areas derived using the GP and VP, respectively.

Isotopologue	n_a	Transition	Band	Position (cm^{-1})	E″ (cm^{-1})	Intensity (cm/molec.)	Type A unc. (‰)	u_δ (‰)	SNR	A_{Diff} (‰)
626	0.98420	*R*66	(30013)←(00001)	6263.369778	1722.9412	3.156E-26	0.03	-	28000:1	10
636	0.01106	*R*50	(30012)←(00001)	6270.249101	994.2387	8.48E-27	0.11	0.33	8900:1	20
628	0.0039471	*R*22	(30012)←(00001)	6269.931712	186.271	1.938E-26	0.09	0.69	10000:1	20
627	0.000734	*P*37	(30012)←(00001)	6265.793803	532.0822	1.403E-27	0.59	0.54	1700:1	40

Figures

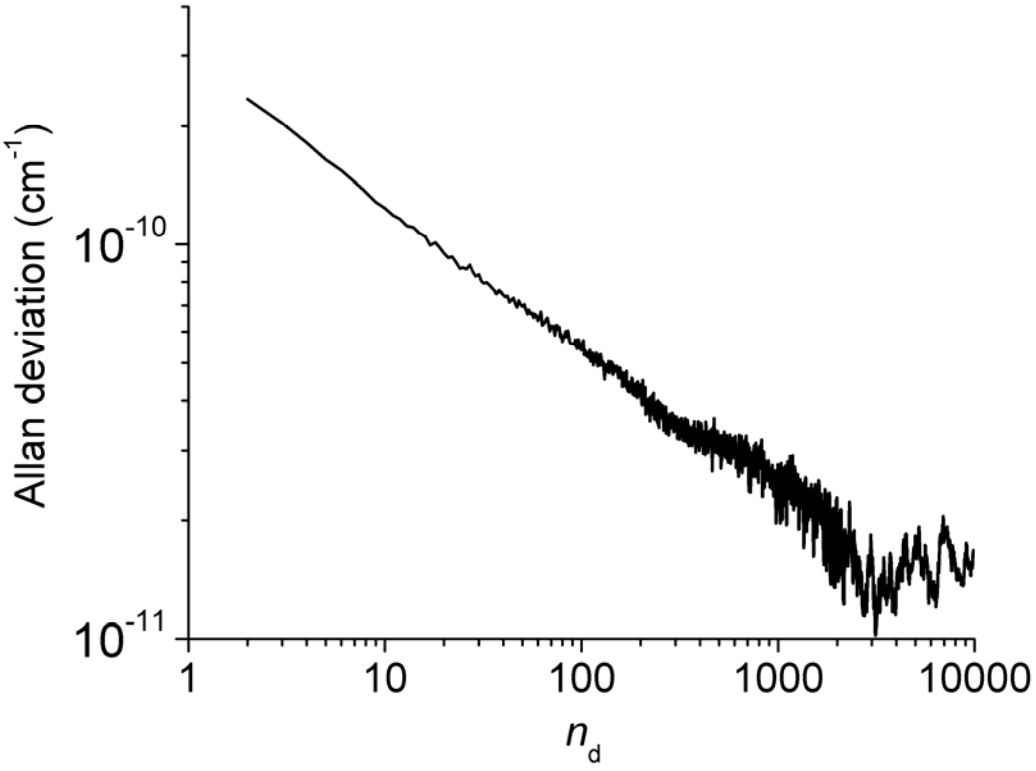

FIGURE 1 Allan deviation (square-root of the Allan variance) of the empty cavity losses as a function of the number of measured ring-down decays, n_d, in an averaging bin. Averaging as many as 3,000 ring-down time constants (at an acquisition rate of 30 Hz) reduces the uncertainty in the absorption coefficient from 2.1×10^{-10} cm^{-1} to 1.5×10^{-11} cm^{-1}, corresponding to a noise-equivalent absorption coefficient of 3.8×10^{-11} cm^{-1} Hz$^{-1/2}$.

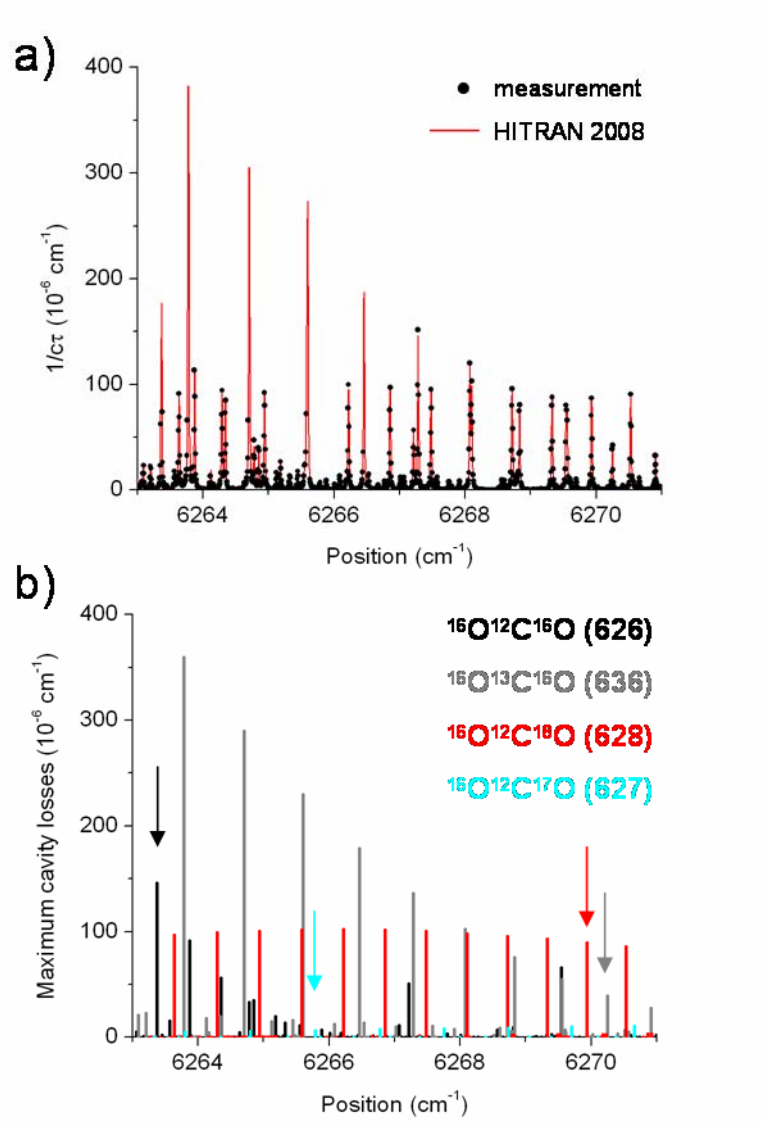

FIGURE 2 Survey of the 6263-6271 cm^{-1} spectral region. a) FS-CRDS measurement (symbols) and calculated HITRAN 2008 spectrum [30] (lines) using the Voigt line profile for a pure CO_2 sample at natural isotopic abundance, a pressure of 6.67 kPa (50 Torr), and a temperature of 298.733 K. b) Corresponding stick spectrum of the four dominant isotopologues calculated through the use of HITRAN 2008. This spectral region was chosen to minimize the absorption difference between isotopologue transitions. Transitions utilized in the present study to determine isotopic ratios are marked by arrows. The $^{16}O^{13}C^{18}O$ transition is unmarked but it is located at 6270.3543 cm^{-1} [30].

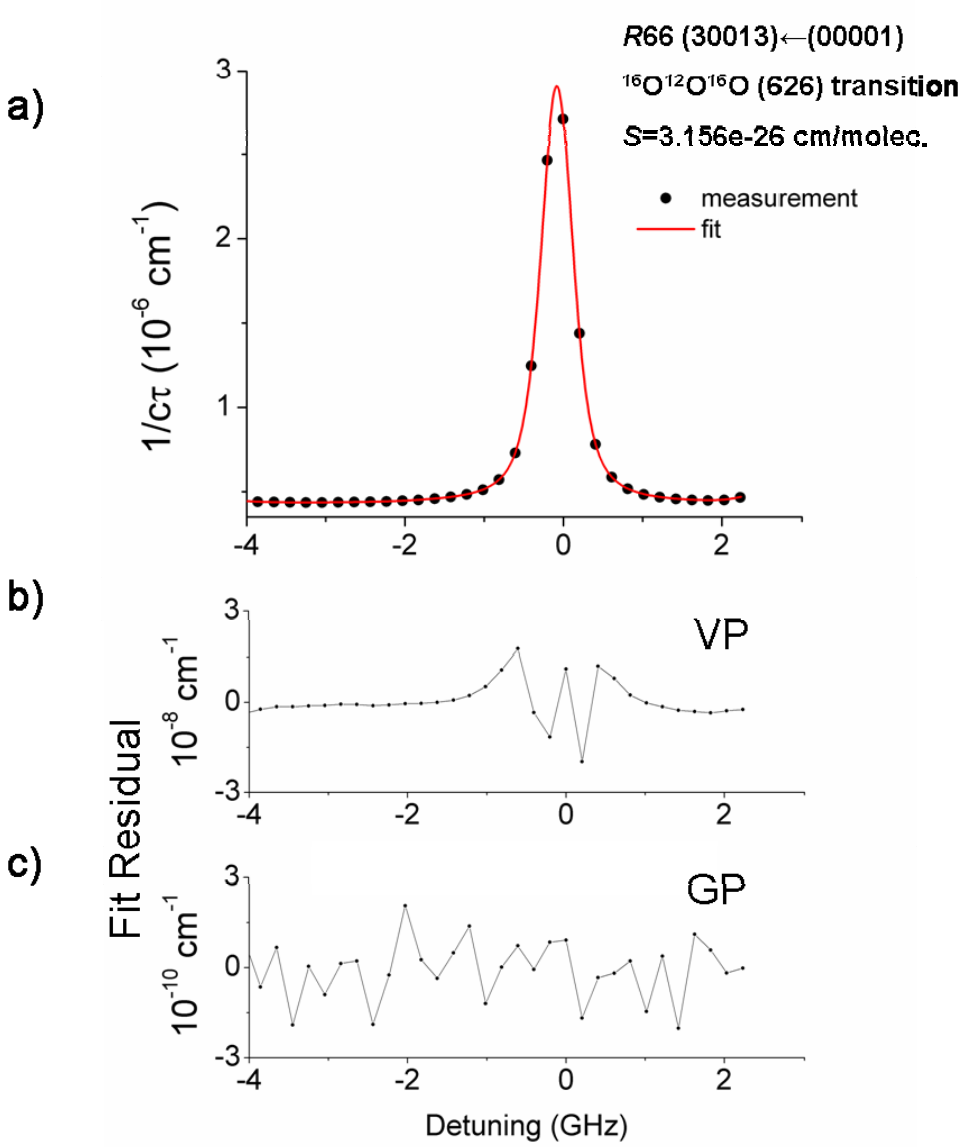

FIGURE 3 a) Measurement and Galatry line profile (GP) fit of the $^{16}O^{12}O^{16}O$ (30013)←(00001) *R*66 transition at 298.929 K and 6.67 kPa (50 Torr) of CO_2 at natural isotopic abundance. This transition is located at 6263.369778 cm^{-1} with an intensity of 3.156×10^{-26} cm $molec.^{-1}$ [30]. b) Voigt line profile (VP) fit residual. All line profile parameters were floated except for the Doppler width which was held fixed. The presence of collisional narrowing leads to a large systematic residual which is ~100 times greater than the instrumental noise level. c) GP fit residual. All line profile parameters were floated except for the Doppler width which was held fixed. Note the difference in scale between the GP and VP fit residuals. The GP accounts for collisional narrowing leading to a signal-to-noise ratio of 28,000:1 with a precision in the area measurement of 0.03‰. The root-mean-square of the Galatry residual is 1×10^{-10} cm^{-1}. The fitted areas determined using the two line profiles differ by 9‰, which is far greater than the measurement precision.

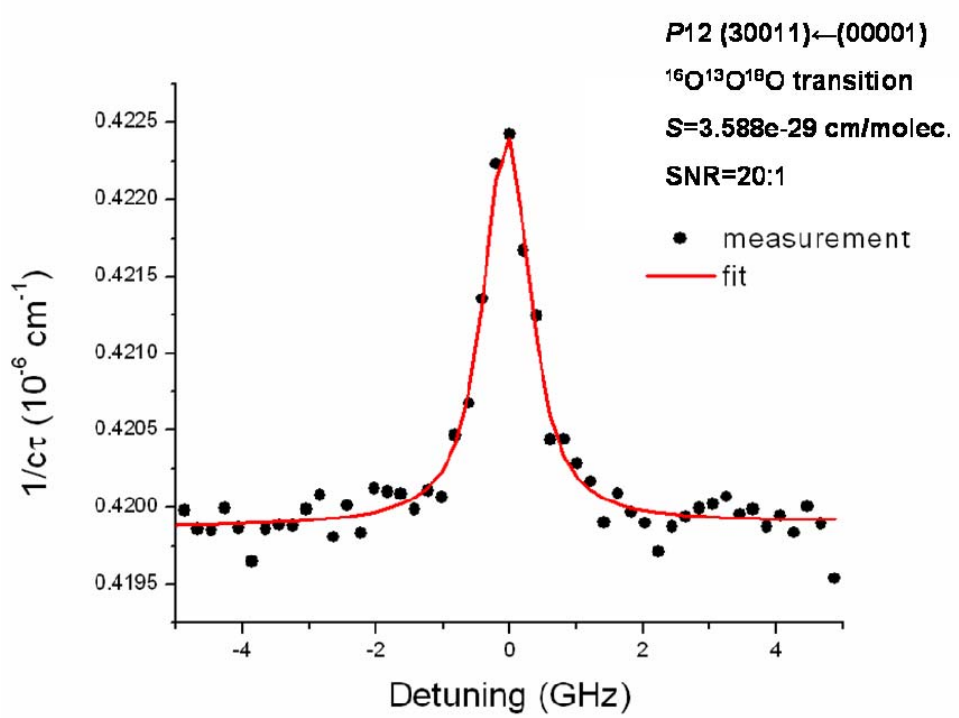

FIGURE 4 Measurement and Galatry fit of the $^{16}O^{13}O^{18}O$ (30011)←(00001) *P*12 transition at 298.814 K and 6.67 kPa (50 Torr) of CO_2 at natural isotopic abundance. This doubly-substituted isotopologue transition is located at 6270.3543 cm^{-1} with an intensity of 3.588×10^{-29} cm molec.$^{-1}$ [30]. In this background subtracted spectrum the signal-to-noise ratio is 20:1.